


Cite this: *RSC Adv.*, 2022, 12, 11877

# Selective monoallylation of anilines to *N*-allyl anilines using reusable zirconium dioxide supported tungsten oxide solid catalyst†

Yoshihiro Kon,<sup>a</sup> Shota Tsurumi,<sup>a</sup> Shunsuke Yamada,<sup>b</sup> Toshiyuki Yokoi<sup>b</sup> and Tadahiro Fujitani<sup>a</sup>

The monoallylation of aniline to give *N*-allyl aniline is a fundamental transformation process that results in various kinds of valuable building block allyl compounds, which can be used in the production of pharmaceuticals and electronic materials. For decades, sustainable syntheses have been gaining much attention, and the employment of allyl alcohol as an allyl source can follow the sustainability due to the formation of only water as a coproduct through dehydrative monoallylation. Although the use of homogeneous metal complex catalysts is a straightforward choice for the acceleration of dehydrative monoallylation, the use of soluble catalysts tends to contaminate products. We herein present a 10 wt% WO<sub>3</sub>/ZrO<sub>2</sub> catalyzed monoallylation process of aniline to give *N*-allyl anilines in good yields with excellent selectivity, which enables the continuous selective flow syntheses of *N*-allyl aniline with 97–99% selectivity. The performed detailed study about the catalytic mechanism suggests that the dispersed WO<sub>3</sub> with the preservation of the W(VI) oxidation state of 10 wt% WO<sub>3</sub>/ZrO<sub>2</sub> with appropriate acidity and basicity is crucial for the monoallylation. The inhibition of the over allylation of the *N*-allyl anilines is explained by the unwilling contact of the *N*-allyl aniline with the active sites of WO<sub>3</sub>/ZrO<sub>2</sub> due to the steric hindrance.

Received 11th January 2022  
Accepted 30th March 2022

DOI: 10.1039/d2ra00198e

rsc.li/rsc-advances

## Introduction

Among various kinds of *N*-allyl compounds,<sup>1</sup> *N*-allyl anilines are known as important building blocks that can add another substituent to N–H and/or allyl moieties to give various value-added fine chemicals, which are applicable to pharmaceuticals and electronic materials.<sup>1–3</sup> While various allylic electrophiles, such as allyl chloride, allyl acetate, and allyl silane, are frequently used in allylation,<sup>4</sup> they contaminate the waste coproducts derived from the chloride, acetate, and silyl substituents of allyl sources. The employment of allyl alcohol (**1**) is a promising pathway to produce *N*-allyl anilines because the resulting coproduct is only water<sup>3,5,6</sup> and the alcohol **1** can be supplied from biomass glycerol by catalytic processes.<sup>7</sup>

The transformation method of **1** with aniline (**2**) to *N*-allyl aniline (**3**) has significantly been studied due to its versatility and broad application.<sup>2,3</sup> There are many examples of the monoallylation of **2** with **1** to produce **3** in excellent yields by

Pd,<sup>8</sup> Ir,<sup>9</sup> Pt<sup>10</sup> and Ni<sup>11</sup> complex catalysts through the formation of  $\pi$ -allyl metal intermediates.<sup>6,8–11</sup> However, these complex catalysts are complicated to treat and costly. Moreover, it is hard to apply metal complex catalysts to practical syntheses because the complex catalysts are solvated and contamination with products. From these perspectives, the expectations of using solid catalysts have been increasing due to the reusability of such catalysts and their applicability to flow reactors.<sup>12,13</sup>

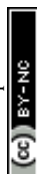
Kaneda and Motokura demonstrated the monoallylation of **1** using Brønsted acidic montmorillonite catalysts, in which the monoallylation of **1** with **2** was performed to give **3** in around 30% yield.<sup>14</sup> However, there are no subsequent reports to increase the yield of **3** with excellent selectivity. Recently, we reported a titanium dioxide supported with molybdenum oxide (MoO<sub>3</sub>/TiO<sub>2</sub>) for the allylation of **2**.<sup>15</sup> However, the MoO<sub>3</sub>/TiO<sub>2</sub>-catalyzed allylation of **2** resulted in **3** with only 4% yield and *N,N*-diallyl aniline (**4**) was formed in 85% yield *via* the formation of an allyl-oxo molybdenum intermediate, which was caused by the reduction of Mo(VI) to Mo(V).<sup>15,16</sup>

To avoid diallylation, we inspired to use tungsten oxide (WO<sub>3</sub>) as a reactive site with the support of metal oxides. WO<sub>3</sub>/ZrO<sub>2</sub> is known as a solid superacid,<sup>17</sup> and there are many useful WO<sub>3</sub>/ZrO<sub>2</sub>-catalyzed reactions, such as alkane isomerization, Friedel–Crafts acylation, alkene trimerization, and biomass conversion.<sup>17,18</sup> However, to the best of our knowledge, there are no examples of the WO<sub>3</sub>/ZrO<sub>2</sub>-catalyzed monoallylation of

<sup>a</sup>Interdisciplinary Research Center for Catalytic Chemistry, National Institute of Advanced Industrial Science and Technology (AIST), 1-1-1 Higashi, Tsukuba, Ibaraki 305-8565, Japan. E-mail: y-kon@aist.go.jp

<sup>b</sup>Nanospace Catalysis Unit, Institute of Innovative Research, Tokyo Institute of Technology, 4259 Nagatsuta, Midori-ku, Yokohama 226-8503, Japan

† Electronic supplementary information (ESI) available. See <https://doi.org/10.1039/d2ra00198e>





anilines utilizing a stable  $W(VI)$  oxidation state of  $WO_3$ . We herein report the development of zirconium dioxide supported with a 10 wt% of  $WO_3$  (10 wt%  $WO_3/ZrO_2$ ), which can catalyze the selective dehydrative monoalkylation of anilines and can be applied to continuous flow reactions.

## Experimental

### Catalyst preparation

The preparation of metal oxide catalysts, such as silicon dioxide supported  $WO_3$  ( $WO_3/SiO_2$ ), aluminum oxide supported  $WO_3$  ( $WO_3/Al_2O_3$ ),  $WO_3/TiO_2$ , magnesium oxide supported  $WO_3$  ( $WO_3/MgO$ ), and  $WO_3/ZrO_2$ , was performed according to a modified impregnation method, where citric acid was used as a pH controlling agent to prevent the formation of tungsten oxide clusters on the surfaces of the supports. For the preparation of 10 wt%  $WO_3/ZrO_2$ , 1.80 g of  $ZrO_2$  were added to a diluted aqueous solution (1 mL) of  $(NH_4)_{10}W_{12}O_{41}(H_2O)_5$  (235.3 mg, 75.1 mmol) with citric acid. The solution was subjected to ultrasonic irradiation for 10 min to ensure a mixture with good homogeneity. After 1 h, the impregnated catalyst was dried at 100 °C for 24 h and then calcined under static air from 25 °C to 500 °C with an increasing rate of 10 °C  $min^{-1}$ . Then, after reaching 500 °C, it was calcined at 500 °C for 3 h.

### Monoalkylation of aniline (2) with allyl alcohol (1) using a $WO_3/ZrO_2$ catalyst (as standard reaction conditions)

A pressure-resistant glass tube equipped with a magnetic stirring bar was loaded with  $WO_3/ZrO_2$  (100 mg), *n*-octane (0.25 mL), **1** (116 mg, 2.0 mmol), and **2** (93.0 mg, 1.0 mmol). The vessel was tightly sealed by a screw cap, and the mixture was stirred (500 rpm) in an oil bath maintained at 140 °C for 24 h. After the reaction, the solution was cooled to room temperature and then diluted with 10 mL of ethyl acetate. Biphenyl (77 mg, 0.50 mmol) was added to the solution as an internal standard for the gas chromatography (GC) analysis. The solution was then placed under ultrasonic irradiation for 10 min to ensure a mixture with good homogeneity. The conversion and yield were determined based on **2** from the analysis of the mixture by GC. The yields of the monoallyl aniline (**3**) and diallyl aniline (**4**) were 71% and 7%, respectively. The conversion of **2** was 78%, and the selectivity of **3** [(yield of **3**)/(conversion of **2**) × 100] was 91%. The isolation of **3** was performed through column chromatography (eluent: *n*-hexane : toluene = 8 : 1) to give **3** with a 58% isolation yield. From an inductively coupled plasma analysis (ICP), the leaching of the W species was found to be 0.35 mg. This value was calculated as 0.4 wt% of the tungsten species in  $WO_3/ZrO_2$  (the calculation was performed by regarding the tungsten species as  $WO_3$ ).

### Retesting of the spent catalyst

The reaction conditions at cycle number 1 (original catalyst) are as follows. **1** (2.0 mmol), **2** (1.0 mmol), and the spent 10 wt%  $WO_3/ZrO_2$  catalyst (100 mg) were stirred in a pressure-resistant glass tube at 140 °C for 24 h. Four batch reactions of the same batch reaction conditions were performed all at once, and the

yields of **3** in the three batch reactions were comparable (average 69% yields). The used  $WO_3/ZrO_2$  was recovered by centrifugation, washed with ethyl acetate, dried at 100 °C for 24 h, and then calcined at 500 °C for 3 h before the next reaction.

### Monoalkylation of aniline (2) with allyl alcohol (1) using a continuous flow reactor for 15 h

A mixture of 10 wt%  $WO_3/ZrO_2$  (1.00 g) and sea sand (1.29 g) (diluent) was packed in a column reactor (length: 100 mm, inner diameter: 5 mm) equipped with a plunger pump, which was used for passing a mixture of **1** (0.2 mol  $L^{-1}$ ), **2** (0.1 mol  $L^{-1}$ ), and biphenyl (0.05 mol  $L^{-1}$ ) to an *n*-octane solution. The reaction was initiated at a flowrate of 0.1 mL  $min^{-1}$  under atmospheric pressure, and the residence time was estimated to be 2.2 min at the column reactor. The column was heated at 140 °C, and the 1.5–6.0 mL solution was corrected each reaction time to check the product yields using GC. The reaction time was set to 0 h when the reaction solution was stabilized to flow. The yields of **3** were in the range of 8–16%, and the selectivities at each reaction time were over 97% from 0 to 15 h.

### Hot filtration test

Hot filtration tests were executed for the reaction mixture of 10 wt%  $WO_3/ZrO_2$  (100 mg), *n*-octane (0.25 mL), **1** (116 mg, 2.0 mmol), and **2** (93.1 mg, 1.0 mmol). The mixture was stirred in a pressure-resistant glass tube at 140 °C and was then temporarily stopped at 4 h. Afterward, the mixture was subjected to quick filtration under reduced pressure, and centrifugation was performed to separate the solid catalysts from the reaction solution. Then, the filtrate was additionally stirred at 140 °C for 4 h without the addition of any new catalysts. The conversion and yield were determined by GC. The yield of **3** was 21%, and the conversion of **2** was 39%. The reaction of **2** at 140 °C for 8 h without hot filtration resulted in **3** with a yield of 48%.

### Materials and methods

**Materials.**  $ZrO_2$  with a specific surface area of 96.4  $m^2 g^{-1}$  (Brunauer–Emmett–Teller surface area (BET)) and commercialized under the name RC-100 was obtained from Daiichi Kigenso Kagaku Kogyo Co., Ltd.  $TiO_2$  P25 with a specific surface area of 62.5  $m^2 g^{-1}$  (BET) and commercialized under the name AEROXIDE  $TiO_2$  P25 was obtained from NIPPON AEROSIL Co., Ltd.  $SiO_2$  with a specific surface area of 105.5  $m^2 g^{-1}$  (BET) was obtained from Catalysis Society of Japan (CSJ) (JCS-SIO-1, a reference catalyst in CSJ), and  $Al_2O_3$  with a specific surface area of 198.7  $m^2 g^{-1}$  (BET) was obtained from Nikki Universal Co., Ltd. (JCS-ALO-6, a reference catalyst in CSJ).  $MgO$  with a specific surface area of 13–19  $m^2 g^{-1}$  (BET) was obtained from Ube Industries, Ltd. (JRC-MGO-3 1000A, a reference catalyst in CSJ). Allyl alcohol, benzyl alcohol, 4-fluoroaniline, 4-bromoaniline, 4-nitroaniline, 1,4-phenylenediamine, 4-methylaniline, 4-*n*-butylaniline, 2-methylaniline, 2,6-dimethylaniline, methyl anthranilate, methyl 2-amino-3-methylbenzoate, and *n*-octane were obtained from Tokyo Chemical Industry Co., Ltd.





(NH<sub>4</sub>)<sub>10</sub>W<sub>12</sub>O<sub>41</sub>(H<sub>2</sub>O)<sub>5</sub>, H<sub>3</sub>PW<sub>12</sub>O<sub>40</sub>(H<sub>2</sub>O)<sub>n</sub>, aniline, 4-chloroaniline, ethyl acetate, biphenyl, *n*-hexane, and CDCl<sub>3</sub> (containing 0.05 wt% of tetramethylsilane (TMS)) were obtained from FUJIFILM Wako Pure Chemical Corporation. H-montmorillonite was obtained from the proton exchange reaction of K-montmorillonite, which was purchased from Kuniimine Industries Co., Ltd. Amberlyst 15DRY was obtained from ORGANO CORPORATION.

**Methods.** GC analyses were performed on a Shimadzu GC-2014 using an Rxi®-1 ms column (0.25 mm × 30 m, GL Sciences Inc). <sup>1</sup>H NMR (400 MHz) and <sup>13</sup>C NMR (400 MHz) spectra were recorded on a Bruker AVANCE 400 spectrometer at 25 °C. The chemical shifts (δ) were in parts per million (ppm) relative to TMS at 0.00 ppm for <sup>1</sup>H and relative to the residual CHCl<sub>3</sub> at 77.0 ppm for <sup>13</sup>C unless otherwise noted. The chemical compositions of the WO<sub>3</sub>/ZrO<sub>2</sub> catalysts were estimated using the ICP (Shimadzu ICPE-9000 spectrometer). N<sub>2</sub> adsorption-desorption measurements were conducted at −196 °C on a MicrotracBEL BELSORP to obtain information on the porosities and mesoporosities. The BET surface area was calculated from the adsorption data with a relative pressure ranging from 0.09 to 0.27. Prior to each adsorption measurement, the sample was evacuated at 200 °C for 6 h. NH<sub>3</sub>-TPD and CO<sub>2</sub>-TPD spectra were recorded on a MicrotracBEL BELCAT II to obtain information on the acidity and basicity of the catalysts, respectively. X-ray diffraction (XRD) patterns were collected using a Rigaku MiniFlex 600 diffractometer equipped with Cu Kα radiation. All the powder samples were scanned over a 2θ range from 10° to 70° with a ratio of 5° min<sup>−1</sup>. High-angle annular dark field scanning mode transmission electron microscopy (HAADF-STEM) and STEM energy dispersive spectroscopy (EDS) analyses were performed using FEI Company Tecnai Osiris. X-ray photoelectron spectroscopy (XPS) measurements were recorded on a VG ESCALab 250 spectrometer fitted with an Al Kα X-ray source (1486.6 eV). The binding energy was based on C 1s (284.6 eV). Elemental analyses were measured on Thermo Fisher Scientific Inc. Flash2000.

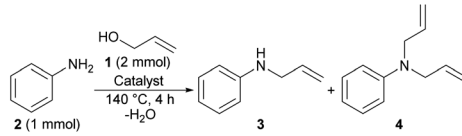
## Results and discussion

### Screening of the catalysts

We screened the catalytic activities of various metal oxide-supported WO<sub>3</sub>, H-montmorillonite, heteropolyacid, and solid acid polymer (Table 1). WO<sub>3</sub> supported by SiO<sub>2</sub>, Al<sub>2</sub>O<sub>3</sub>, TiO<sub>2</sub>, MgO, and ZrO<sub>2</sub> were prepared using the modified impregnation method, as shown in the experimental section. The crystal structures of WO<sub>3</sub>/SiO<sub>2</sub>, WO<sub>3</sub>/Al<sub>2</sub>O<sub>3</sub>, WO<sub>3</sub>/TiO<sub>2</sub>, WO<sub>3</sub>/MgO, and WO<sub>3</sub>/ZrO<sub>2</sub> were checked using XRD analyses to confirm the preservation of their support metal oxide crystal structures (Fig. S1†). In the XRD, there were no characteristic signals of 2θ = 23.2, 23.7, and 24.4°, which are generally assigned to the WO<sub>3</sub> monoclinic crystal structures.<sup>19</sup> Therefore, the prepared WO<sub>3</sub>/SiO<sub>2</sub>, WO<sub>3</sub>/Al<sub>2</sub>O<sub>3</sub>, WO<sub>3</sub>/TiO<sub>2</sub>, WO<sub>3</sub>/MgO, and WO<sub>3</sub>/ZrO<sub>2</sub> showed the dispersed WO<sub>3</sub> nature on the surface of the solid catalysts.

Table 1 indicates the results of the dehydrative monoallylation of 2 with 1 in the presence of various solid catalysts at 140 °C for 4 h. Although solid acids such as WO<sub>3</sub>/SiO<sub>2</sub>, WO<sub>3</sub>/

Table 1 Monoallylation of 1 with 2 using heterogeneous catalysts<sup>a</sup>



Entry	Catalyst (100 mg)	Conv. of 2 <sup>b</sup> (%)	Yields <sup>b</sup> (%)		Selectivity <sup>c</sup> (%)
			3	4	
1	10 wt% WO <sub>3</sub> /SiO <sub>2</sub>	11	4	0	36
2	10 wt% WO <sub>3</sub> /Al <sub>2</sub> O <sub>3</sub>	11	2	0	18
3	10 wt% WO <sub>3</sub> /TiO <sub>2</sub>	15	6	0	40
4	10 wt% WO <sub>3</sub> /MgO	7	0	0	0
5	10 wt% WO <sub>3</sub> /ZrO <sub>2</sub>	38	31	0.6	82
6	WO <sub>3</sub>	6	1	0	17
7	ZrO <sub>2</sub>	5	0	0	0
8	—	4	0	0	0
9	H-montmorillonite	23	5	0	22
10	H <sub>3</sub> PW <sub>12</sub> O <sub>40</sub> (H <sub>2</sub> O) <sub>n</sub>	18	2	0	13
11	Amberlyst 15DRY	50	0	0	0

<sup>a</sup> Reaction conditions: 1 (2.0 mmol), 2 (1.0 mmol), solid catalyst (100 mg), *n*-octane (0.25 mL), 140 °C, 500 rpm, 4.0 h, unless otherwise stated. <sup>b</sup> Conversion and yield were on the basis of 2, determined by GC analysis using biphenyl as an internal standard. <sup>c</sup> Selectivity = (yield of 3)/(conversion of 2) × 100 (%).

Al<sub>2</sub>O<sub>3</sub>, and WO<sub>3</sub>/TiO<sub>2</sub> were estimated to be reactive solid acids,<sup>17</sup> they gave 3 in only 2–6% of the yields with low selectivity (Table 1, entries 1–3). In the case of using the WO<sub>3</sub>/MgO catalyst, in which MgO is known as a basic support, the allylation of 2 did not proceed (Table 1, entry 4). Only the case of using WO<sub>3</sub>/ZrO<sub>2</sub> indicated good reactivity to give 3 in 31% yield with 82% selectivity, and the coproduction of 4 was given in only 0.6% yield (Table 1, entry 5). When the reactions were performed with WO<sub>3</sub> or ZrO<sub>2</sub> only, they did not proceed (Table 1, entries 6 and 7). Also, the reactions did not proceed without catalysts (Table 1, entry 8). H-montmorillonite, which is known as an effective solid acid catalyst,<sup>14</sup> gave 3 in 5% yield, and the heteropolyacid (H<sub>3</sub>PW<sub>12</sub>O<sub>40</sub>(H<sub>2</sub>O)<sub>n</sub>) catalyst<sup>20</sup> resulted in the production of 3 in 2% yield (Table 1, entries 9 and 10). Amberlyst 15DRY, as an example of solid acid polymers that contain −SO<sub>3</sub>H groups on the surface,<sup>21</sup> showed 50% conversion of 2 without the detection of any products by GC analysis because aniline was adsorbed on its surface (Table 1, entry 11).<sup>22</sup> The adsorption of 2 on the catalyst surface was also estimated for other solid catalysts (Table 1, entries 1–3, 9 and 10).

### Effect of supports (SiO<sub>2</sub>, Al<sub>2</sub>O<sub>3</sub>, TiO<sub>2</sub>, and ZrO<sub>2</sub>)

The screening data with the BET surface area, acid amounts measured by NH<sub>3</sub>-TPD, acid density calculated from the BET surface area, and acid amounts of 10 wt% WO<sub>3</sub>/SiO<sub>2</sub>, 10 wt% WO<sub>3</sub>/Al<sub>2</sub>O<sub>3</sub>, 10 wt% WO<sub>3</sub>/TiO<sub>2</sub>, and 10 wt% WO<sub>3</sub>/ZrO<sub>2</sub> are shown in Table 2. As shown in the correlation between the acid densities and yields of 3, 10 wt% WO<sub>3</sub>/ZrO<sub>2</sub> showed





**Table 2** BET surface area, acid amounts, acid density, conversion of **2** and yield of **3** from the monoallylation of **2** using WO<sub>3</sub>/SiO<sub>2</sub>, WO<sub>3</sub>/Al<sub>2</sub>O<sub>3</sub>, WO<sub>3</sub>/TiO<sub>2</sub> and WO<sub>3</sub>/ZrO<sub>2</sub>

Catalysts <sup>a</sup>	BET (m <sup>2</sup> g <sup>-1</sup> )	Acid amount (mmol g <sup>-1</sup> )	Acid density <sup>b</sup> (mmol m <sup>-2</sup> )	Yield of <b>3</b> <sup>c,d</sup> (%)
WO <sub>3</sub> /SiO <sub>2</sub>	99	0.195	$1.97 \times 10^{-3}$	4
WO <sub>3</sub> /Al <sub>2</sub> O <sub>3</sub>	178	0.364	$2.04 \times 10^{-3}$	2
WO <sub>3</sub> /TiO <sub>2</sub>	55	0.221	$4.02 \times 10^{-3}$	6
WO <sub>3</sub> /ZrO <sub>2</sub>	105	0.301	$2.87 \times 10^{-3}$	31

<sup>a</sup> 10 wt% WO<sub>x</sub> was supported. <sup>b</sup> Acid density = (acid amount)/BET. <sup>c</sup> Reaction conditions: **1** (2.0 mmol), **2** (1.0 mmol), catalyst (100 mg), 140 °C, 500 rpm, 4.0 h. <sup>d</sup> Yields were on the basis of **2**, determined by GC analysis using biphenyl as an internal standard.

a specifically high yield (Fig. S2†). Although 10 wt% WO<sub>3</sub>/TiO<sub>2</sub> showed a higher acid density than that of 10 wt% WO<sub>3</sub>/ZrO<sub>2</sub>, it produced **3** in only 6% yield. Comparing the acid strengths of 10 wt% WO<sub>3</sub>/TiO<sub>2</sub> and 10 wt% WO<sub>3</sub>/ZrO<sub>2</sub> by NH<sub>3</sub>-TPD, a signal derived from a relatively strong acid at 300 to 500 °C was observed in 10 wt% WO<sub>3</sub>/ZrO<sub>2</sub>, but hardly observed in 10 wt% WO<sub>3</sub>/TiO<sub>2</sub> (Fig. S3†). The moderate acid density with relatively strong acid of 10 wt% WO<sub>3</sub>/ZrO<sub>2</sub> was effective in proceeding the monoallylation of **2**. The dispersed tungsten species in 10 wt% WO<sub>3</sub>/ZrO<sub>2</sub> was checked by HAADF-STEM EDS mappings as well as XRD patterns, as shown in Fig. S1,† where the WO<sub>3</sub>/ZrO<sub>2</sub> catalyst showed well-dispersed tungsten species with a particle size of under 4 nm (Fig. S4†).

### Screening the amount of tungsten oxides in WO<sub>3</sub>/ZrO<sub>2</sub>

Next, the correlation between the amounts of WO<sub>3</sub> in the WO<sub>3</sub>/ZrO<sub>2</sub> catalyst and their reactivities was investigated using the 1, 2.5, 5, 7.5, and 10 wt% WO<sub>3</sub>/ZrO<sub>2</sub> catalysts (Fig. 1).

The characteristic sharp signals of the WO<sub>3</sub> monoclinic crystal structures were not observed at the XRD spectra of all the employed WO<sub>3</sub>/ZrO<sub>2</sub> catalysts, which shows the good dispersion nature of WO<sub>3</sub> on the ZrO<sub>2</sub> surface (highlighted in pale blue, Fig. 1a).<sup>19</sup> The characteristic patterns assigned to the monoclinic ZrO<sub>2</sub> structure in the XRD spectra were shown (Fig. 1a).<sup>19</sup> The WO<sub>3</sub> surface density is known to be a good indicator to express the surface structures in WO<sub>3</sub>/ZrO<sub>2</sub> catalysts.<sup>19,23</sup> We calculated the WO<sub>3</sub> surface density of the prepared 1, 2.5, 5, 7.5, and 10 wt% WO<sub>3</sub>/ZrO<sub>2</sub> from the ICP and BET data, and the calculated values were found to be 0.48, 0.81, 1.43, 2.11, and 2.59 W nm<sup>-2</sup>, respectively (Table S1†).<sup>23</sup> The correlation between the WO<sub>3</sub> surface density and the yields of **3** is shown in Fig. 1b.

All the catalyst samples were distributed in the WO<sub>3</sub> surface density range of 0–3 W nm<sup>-2</sup>, which indicates that there were no WO<sub>3</sub> crystallites and that less W–O–W bonds were formed on the surface of the employed WO<sub>3</sub>/ZrO<sub>2</sub>.<sup>19a</sup> Also, the WO<sub>3</sub> surface density range below 4 W nm<sup>-2</sup> shows that the surface WO<sub>3</sub> were in the levels of monolayer coverage.<sup>19b</sup> The WO<sub>3</sub> species in the range below 4 W nm<sup>-2</sup> are reported to be stabilized through multiple W–O–Zr bonds between each WO<sub>6</sub> octahedra and the ZrO<sub>2</sub> surface.<sup>19</sup> Also, the increase in the WO<sub>3</sub> surface density corresponded to the increase in the W–OH–Zr active acidic sites.<sup>19</sup> Moreover, the yield of **3** was saturated at over 2.11 W nm<sup>-2</sup> for 24 h (hollow red circle, Fig. 1b). However, the

selectivity of **3** was improved when the WO<sub>3</sub> surface density of WO<sub>3</sub>/ZrO<sub>2</sub> increased from 2.11 to 2.59 W nm<sup>-2</sup> (hollow blue diamonds, Fig. 1b). This data can be explained by considering the balance of the acidic sites and basic sites of WO<sub>3</sub>/ZrO<sub>2</sub>. ZrO<sub>2</sub> is known to show the bifunctional characters of relatively stable solid acids and solid bases,<sup>24</sup> and the basic sites would adsorb **2** through the hydrogen bonding between H–N and the basic surface of ZrO<sub>2</sub>. An increase in the WO<sub>3</sub> surface density signifies an increase in the W–OH–Zr active acidic sites, which results in a relative decrease in the basic sites of ZrO<sub>2</sub>. A decrease in the basic sites of ZrO<sub>2</sub> was observed by CO<sub>2</sub>-TPD (Table S1, Fig. S5†). The presence of basic sites in WO<sub>3</sub>/ZrO<sub>2</sub> was effective for the acceleration of the monoallylation process because of the

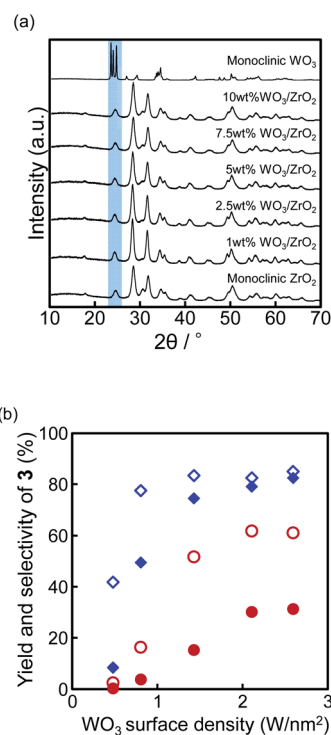


**Fig. 1** (a) XRD patterns of 1, 2.5, 5, 7.5 and 10 wt% WO<sub>3</sub>/ZrO<sub>2</sub> species. Pale blue highlight shows the WO<sub>3</sub> monoclinic characteristic patterns; (b) correlation between the W surface density (W nm<sup>-2</sup>) and the yields (selectivities) of **3**. Yields and selectivities at 4 h were indicated by the solid red circle and solid blue diamond, respectively. Yields and selectivities at 24 h were indicated by the hollow red circle and hollow blue diamond, respectively.





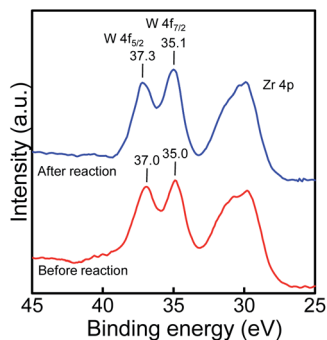


Fig. 2 XPS image of  $\text{WO}_3/\text{ZrO}_2$  before and after the monoallylation.

adsorption of **2** to the basic sites on the catalyst surface. However, the presence of excess basic sites reduced selectivity because **2** was strongly adsorbed on the basic sites and could not be recovered from  $\text{WO}_3/\text{ZrO}_2$ . From these aspects, the optimized  $\text{WO}_3$  surface density on 10 wt%  $\text{WO}_3/\text{ZrO}_2$  showing  $2.59 \text{ W nm}^{-2}$  supplied appropriate distribution of the acid and basic active sites on the 10 wt%  $\text{WO}_3/\text{ZrO}_2$ , which were crucial for proceeding the highly selective monoallylation of **2**.

The measurement of the  $\text{W } 4f_{7/2}$  and  $4f_{5/2}$  profiles of 10 wt%  $\text{WO}_3/\text{ZrO}_2$  was performed by the XPS (Fig. 2). By referencing to  $\text{C } 1s$  (284.6 eV), the peaks at the 35.0 eV and 37.0 eV binding energies (BEs) were ascribed to  $\text{W } 4f_{7/2}$  and  $4f_{5/2}$ , which were corresponding to  $\text{W(VI)}$ .<sup>25</sup> After the reaction, the peaks slightly changed (35.1 eV and 37.3 eV for  $\text{W } 4f_{7/2}$  and  $4f_{5/2}$ , respectively) with the same shape of the spectra, and the lower BEs assigned to  $\text{W(V)}$  and  $\text{W(IV)}$  were not observed at all. From the XPS analysis, we confirmed that the oxidation state of tungsten(vi) did not change during the reaction.

### Optimization of the reaction conditions using the $\text{WO}_3/\text{ZrO}_2$ catalyst

The developed 10 wt%  $\text{WO}_3/\text{ZrO}_2$ -catalyzed monoallylation was optimized by adjusting the solvents, reaction temperature, and reaction time (Tables S2, S3† and 3). The monoallylation of **2** was inhibited using polar solvents, such as ketone, amide, and ether, to give **3** in 0–12% yields (Table S2†). However, the alkanes and aromatic solvents showed good reactivity for the monoallylation of **2** to give **3** in 25–32% yields (Table S2†). The reactivity decreased under solvent-free conditions to give **3** in 13% yield (Table S2†). The yields of **3** increased from 14% to 67% with increasing the reaction temperature from 130 to 160 °C, respectively (Table S3†). We selected the reaction temperature of 140 °C for the monoallylation process because the reaction over 150 °C caused the formation of the undesired product **4**.

The time course reaction profile of the allylation using 10 wt%  $\text{WO}_3/\text{ZrO}_2$  showed steady progress of forming **3** until 8 h. Then, the reaction proceeded slowly to reach 71% yield for 24 h (Table 3). The selectivity of **3** was maintained over 80% at 8 h and 24 h, and the slight decrease in the selectivity of **3** was observed at 48 h because of the increase of **4**. The allylation of the mixture of **1** (1.5 mmol), **2** (0.5 mmol), and **3** (0.5 mmol) was

Table 3 Screening of the reaction time of monoallylation of **2** using 10 wt%  $\text{WO}_3/\text{ZrO}_2$ <sup>a</sup>

Reaction time (h)	Conversion of <b>2</b> <sup>b</sup> (%)	Yield of <b>3</b> <sup>b</sup> (%)	Yield of <b>4</b> <sup>b</sup> (%)	Selectivity <sup>c</sup> (%)
2	22	14	0	66
4	32	25	0	79
8	57	48	2	85
24	78	71	7	91
48	87	70	10	80

<sup>a</sup> The base reaction conditions are as follows: **1** (2.0 mmol), **2** (1.0 mmol), 10 wt%  $\text{WO}_3/\text{ZrO}_2$  (100 mg), *n*-octane (0.25 mL), 140 °C, 500 rpm, 4.0 h. <sup>b</sup> Determined by GC analysis based on **2**, the yields are the average of the results of three experiments. <sup>c</sup> Selectivity = (yield of **3**)/(conversion of **2**) × 100 (%).

performed as a competitive reaction of **2** and **3** (Scheme S1†). After 4 h, products with a molar ratio of **2** : **3** : **4** = 0.33 : 0.66 : 0.02 were observed, and the ratio of the products reached **2** : **3** : **4** = 0.18 : 0.71 : 0.05 (mmol) at 24 h (Scheme S1†). The results indicated that **2** was more reactive than **3**, and were in good agreement with the production of **3** in 71% yield with 91% selectivity, as shown in Table 3 and Fig. 1. A catalytic reaction was assumed to have proceeded on the surface of the solid catalyst since the reaction was terminated when the catalyst was removed by hot filtration during the reaction (Table S4†).

### Reuse of $\text{WO}_3/\text{ZrO}_2$ and continuous synthesis using $\text{WO}_3/\text{ZrO}_2$

The developed 10 wt%  $\text{WO}_3/\text{ZrO}_2$  was easily separated from the reaction solution, and it could be reused at least three times before seeing a significant loss in yields of **3** (Table S5 and Fig. S6†). Continuous flow monoallylation of **2** with **1** was demonstrated using a flow reactor equipped with a glass column (length: 100 mm, inner diameter: 5 mm) and packed with 10 wt%  $\text{WO}_3/\text{ZrO}_2$ , which was diluted with sea sand (Fig. 3).

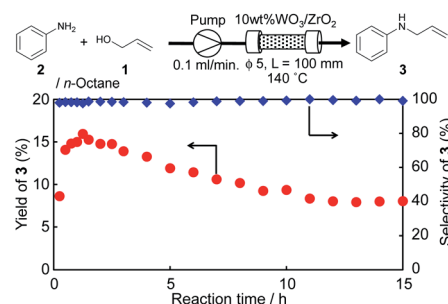
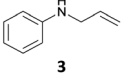
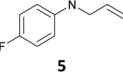
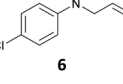
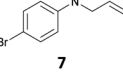
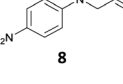
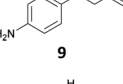
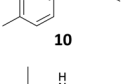
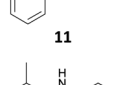
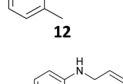
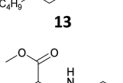
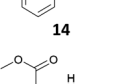
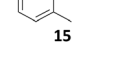


Fig. 3 Monoallylation of **2** with **1** in the presence of  $\text{WO}_3/\text{ZrO}_2$  using a flow reactor.





**Table 4** Monoallylation of various anilines using 10 wt% WO<sub>3</sub>/ZrO<sub>2</sub><sup>a</sup>

$\text{R-NH}_2 \quad + \quad \text{HO-CH}_2\text{-CH=CH}_2 \xrightarrow[140^\circ\text{C, 24 h}]{10\text{wt\%WO}_3/\text{ZrO}_2, -\text{H}_2\text{O}} \text{R-NH-CH}_2\text{-CH=CH}_2$ (1 mmol)                      1 (2 mmol)		
Products	Yields <sup>b</sup> (%) of <i>N</i> -allyl anilines	Selectivity (mono : di) <sup>c</sup> (%)
	58	98
	33	97
	43	96
	45	98
	25	96
	30	— <sup>d</sup>
	29	97
	54	95
	17	94
	29	— <sup>d</sup>
	63	— <sup>d</sup>
	29	— <sup>d</sup>

<sup>a</sup> Reaction conditions: **1** (2.0 mmol), aniline (1.0 mmol), WO<sub>3</sub>/ZrO<sub>2</sub> (100 mg), *n*-octane (0.25 mL), 140 °C, 24 h. <sup>b</sup> Isolated yield. <sup>c</sup> Selectivity (mono : di) = ((isolated yield of *N*-allyl aniline)/[(isolated yield of *N*-allyl aniline) + (isolated yield of *N,N*-diallyl aniline)]) × 100 (%). <sup>d</sup> Small amounts of the other compounds were contaminated.

A mixture of **1** and **2** in an *n*-octane solution was sent to the catalyst column at a flow rate of 0.1 mL min<sup>-1</sup> under atmospheric pressure. Continuous flow synthesis of **3** was performed at 140 °C for 15 h, and **3** was continuously produced in around 10–15% yields with 97–99% selectivity without detection of **4**

(Fig. 3 and Table S6†). The estimated contact time in the catalyst column was 2.2 min, and the calculated TOF per W was around 20 (h<sup>-1</sup>).<sup>19,26</sup>

### Scope and limitation of the substrates

The developed 10 wt% WO<sub>3</sub>/ZrO<sub>2</sub> catalyzed the monoallylation of various anilines with **1** (Table 4). Besides **2**, the 4-fluoro-, 4-chloro-, and 4-bromo-substituted anilines reacted with **1** in the presence of the 10 wt% WO<sub>3</sub>/ZrO<sub>2</sub> catalyst to give the corresponding *N*-allyl anilines **3**, **5**, **6**, and **7** in 58, 33, 43, and 45% isolated yields, respectively (Table 4). The electron-deficient substrates, such as the 4-nitro-substituted aniline, decreased the reactivity to give **8** in 25% yield. The monoallylation of the 4-amino-substituted aniline gave **9** in 30% yield without the production of *N,N'*-diallyl aniline. Also, the allylation of the 4-methyl-, 2-methyl-, and 2,6-dimethyl anilines gave the corresponding *N*-allyl anilines **10**, **11** and **12** in 29, 54, and 17% yields, respectively. The electronic effects at the 4-position of the anilines were less correlated with the isolated yields of the *N*-allyl anilines (Table 3, **3** and **5–10**). On the other hand, the sterically bulky 2,6-dimethyl aniline showed lower reactivity than that of the 2-methyl aniline (Table 3, **11** and **12**). The elongation of the alkyl chain at the 4-position from the methyl to *n*-butyl in the aniline did not affect the reactivity to give **13** in 29% yield. Various *N*-allyl anilines were selectively synthesized at the molar ratio of **1** : aniline = 2 : 1, and the selectivity (mono : di) of *N*-allyl anilines were calculated to be over 94% (Table 4).

The steric effect is clearly shown in the comparison of the syntheses of **14** and **15**. The monoallylation of methyl anthranilate gave **14** in 63% yield, which indicated that the reactivity did not reduce because monoallylation occurred at the sterically less hindered N–H bond. In addition, the stabilization by the intramolecular hydrogen bonding between the carbonyl oxygen and hydrogen at H–N accelerated the monoallylation of the aniline with the stabilization of the given **14**. On the contrary, the reaction of the methyl 2-amino-3-methylbenzoate with **1** showed the low yield of **15** in 29% yield. This was because the reaction site of the aniline was sterically hindered by the methyl substituent at the 3-position of the methyl benzoate.

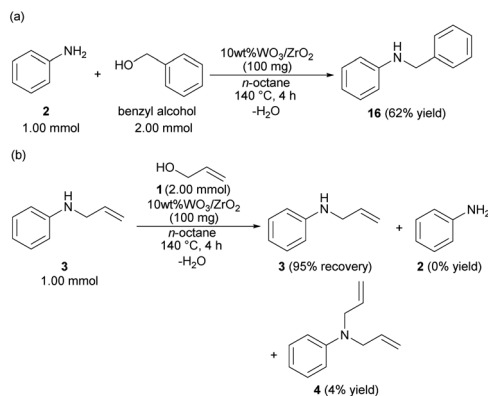
The reaction was not affected by atmospheric conditions. The average yields of **3** in the two experiments were 64% (under Ar) and 61% (under air), respectively (Table S7†). The developed 10 wt% WO<sub>3</sub>/ZrO<sub>2</sub> catalyst did not show any reactivity for the *N*-allylation of the aliphatic amines, such as *n*-propyl amine, *n*-dodecyl amine, benzylamine, and cyclohexylamine, because they would be strongly adsorbed on the 10 wt% WO<sub>3</sub>/ZrO<sub>2</sub> catalyst to deactivate the W–OH–Zr active acidic sites (Table S8†). Also, the developed 10 wt% WO<sub>3</sub>/ZrO<sub>2</sub> catalyst did not apply to the selective monoallylation using other allylic alcohols, for example, the reaction using *trans*-2-buten-1-ol instead of **1** resulted in the formation of complex mixtures.

### Reaction mechanism

The reaction mechanism was considered based on the probe experiments and the screening of the anilines. Benzyl alcohol







**Scheme 1** Probe experiments using 10 wt% WO<sub>3</sub>/ZrO<sub>2</sub>; (a) reaction of 2 with benzyl alcohol; (b) reaction of 3 with 1.

reacted with 2 to give benzyl aniline (16) in 62% yield (Scheme 1(a)). The developed catalytic reaction was not only allowed to 1 but also allowed to the electron-deficient carbon compounds such as benzyl alcohol by the nucleophilic attack of the N-atom of 2. The allylation of 3 with 1 at 140 °C for 4 h did not give 4 in good yield, but the recovery of 3 was observed in 95% yield (Scheme 1(b)). The steric repulsion between the allyl moiety of 3 and the surface of 10 wt% WO<sub>3</sub>/ZrO<sub>2</sub> hindered over allylation.

The employed 10 wt% WO<sub>3</sub>/ZrO<sub>2</sub> catalyst was estimated to form W–OH–Zr structures on its surface (Fig. 1).<sup>19a,b</sup> Besides, the support ZrO<sub>2</sub> is known to work as a bifunctional solid acid and solid base.<sup>24</sup> From these aspects with the probe reactions and the screening of the anilines, the allylation process seemed to proceed through the nucleophilic attack of the N-atom of 2 to the allyl moiety of 1.

Also, the activation of the N-atom of 2 by the basic site of ZrO<sub>2</sub> and the activation of the allyl moiety of 1 by the Brønsted acidic site of W–OH–Zr would be effective in accelerating the nucleophilic attack of 2 (Fig. 4a). Therefore, 3 did not proceed the allylation with 1, as 3 could not access the surface of ZrO<sub>2</sub> due to the steric repulsion between its allyl moiety and the surface of 10 wt% WO<sub>3</sub>/ZrO<sub>2</sub> (Fig. 4b). In the case of MoO<sub>3</sub>/TiO<sub>2</sub>, the allyl-oxo molybdenum species had high nucleophilicity to receive the attack from the N-atom of 2 without any activation of aniline.<sup>15</sup> However, 10 wt% WO<sub>3</sub>/ZrO<sub>2</sub> did not form an allyl-oxo tungstate intermediate. And a direct contact between aniline and ZrO<sub>2</sub> was needed for proceeding the allylation process. Therefore, the hindered random surface structure of 10 wt% WO<sub>3</sub>/ZrO<sub>2</sub> directly affected the selective synthesis of 3 (Fig. 4).

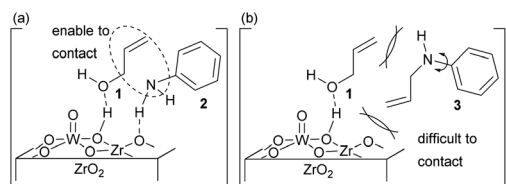


**Fig. 4** Active sites of 10 wt% WO<sub>3</sub>/ZrO<sub>2</sub> during the allylation of (a) 2 with 1 and (b) 3 with 1.

## Conclusions

In this study, selective dehydrative monoallylation of anilines was performed by using optimized amounts of WO<sub>3</sub> supported with a ZrO<sub>2</sub> catalyst (10 wt% WO<sub>3</sub>/ZrO<sub>2</sub>). Due to the preservation of the optimized acid density of the WO<sub>3</sub> on ZrO<sub>2</sub> and the support of the basic sites on ZrO<sub>2</sub> during the monoallylation process, 10 wt% WO<sub>3</sub>/ZrO<sub>2</sub> could catalyze the allylation of 2 to give a corresponding monoallyl aniline 3 up to 78% yield with 93% selectivity. The developed 10 wt% WO<sub>3</sub>/ZrO<sub>2</sub> catalyst could proceed the monoallylation process in a fixed-bed flow reactor for 15 hours to continuously produce 3 with over 97% selectivity. From the performed XPS analyses before and after the reaction, the preservation of WO<sub>3</sub> with the W(VI) oxidation state was confirmed during the allylation process. Considering the probe reactions and substrate scope, the steric repulsion between the allyl substituent of the monoallyl aniline and the random structure of the 10 wt% WO<sub>3</sub>/ZrO<sub>2</sub> surface prevented the over allylation of the monoallyl aniline.

## Author contributions

Conceptualization, investigation, and writing, Y. K.; investigation, S. T. and S. Y. formal analysis, T. Y.; supervision and formal analysis, T. F.

## Conflicts of interest

There are no conflicts to declare.

## Acknowledgements

This article is partly based on results obtained from a project, JPNP20005, subsidized by the New Energy and Industrial Technology Development Organization (NEDO), Japan. We express our thanks to Mr Takuya Nakashima and Mr Makoto Kitai for useful discussion.

## Notes and references

- (a) M. Johannsen and K. A. Jørgensen, *Chem. Rev.*, 1998, **98**, 1689; (b) L. Kräling, J. Krey, G. Jakobson, J. Grolig and L. Miksche, "Allyl Compounds" *Ullmann's Encyclopedia of Industrial Chemistry*, Wiley-VCH, Weinheim, 2000.
- Recent examples of transformations from monoallyl anilines, see: (a) H. Egami, S. Kawamura, A. Miyazaki and M. Sodeoka, *Angew. Chem., Int. Ed.*, 2013, **52**, 7841; (b) S. Das, F. D. Bobbink, G. Laurency and P. J. Dyson, *Angew. Chem., Int. Ed.*, 2014, **53**, 12876; (c) X.-F. Liu, X.-Y. Li, C. Qiao, H.-C. Fu and L.-N. He, *Angew. Chem., Int. Ed.*, 2017, **56**, 7425; (d) W. Li, J. K. Boon and Y. Zhao, *Chem. Sci.*, 2018, **9**, 600; (e) S. Mukherjee and B. List, *J. Am. Chem. Soc.*, 2007, **129**, 11336.
- J. Muzurt, *Eur. J. Org. Chem.*, 2007, 3077.
- (a) B. M. Trost and D. L. Van Vranken, *Chem. Rev.*, 1996, **96**, 395; (b) J. Tsuji, *Palladium Reagents and Catalysts: New Perspectives for the 21st Century*, Wiley, Chichester, 2004; (c)





- V. Pace, F. Martínez, M. Fernández, J. V. Sinisterra and A. R. Alcántara, *Org. Lett.*, 2007, **9**, 2661.
- 5 Y. Tamaru, *Eur. J. Org. Chem.*, 2005, 2647.
- 6 (a) B. Sundararaju, M. Achard and C. Bruneau, *Chem. Soc. Rev.*, 2012, **41**, 4467; (b) M. Bandini, G. Cera and M. Chiarucci, *Synthesis*, 2012, **44**, 504.
- 7 For recent reviews for the formation of allyl alcohol from glycerol, see: (a) S. Raju, M.-E. Moret and R. J. M. K. Gebbink, *ACS Catal.*, 2015, **5**, 281; (b) J. R. Dethlefsen and P. Fristrup, *ChemSusChem*, 2015, **8**, 767.
- 8 (a) F. Ozawa, H. Okamoto, S. Kawagishi, S. Yamamoto, T. Minami and M. Yoshifuji, *J. Am. Chem. Soc.*, 2002, **124**, 10968; (b) M. Kimura, M. Futamata, K. Shibata and Y. Tamaru, *Chem. Commun.*, 2003, 234; (c) H. Kinoshita, H. Shinokubo and K. Oshima, *Org. Lett.*, 2004, **6**, 4085; (d) S.-C. Yang, C.-L. Yu and Y.-C. Tsai, *Tetrahedron Lett.*, 2000, **41**, 7097; (e) G. Mora, B. Deschamps, S. van Zutphen, X. F. le Goff, L. Ricard and P. le Floch, *Organometallics*, 2007, **26**, 1846; (f) C. Thoumazet, H. Grutzmacher, B. Deschamps, L. Ricard and P. le Floch, *Eur. J. Inorg. Chem.*, 2006, 3911; (g) Y. S. Wagh, D. N. Sawant, K. P. Dhake and B. M. Bhanage, *Catal. Sci. Technol.*, 2012, **2**, 835; (h) J. A. van Rijn, A. den Dunnen, E. Bouwman and E. Drent, *J. Mol. Catal. A: Chem.*, 2010, **329**, 96; (i) Y. Tao, Y. Zhou, J. Qu and M. Hidai, *Tetrahedron Lett.*, 2010, **51**, 1982; (j) I. Šolić, D. Reich, J. Lim and R. W. Bates, *Asian J. Org. Chem.*, 2017, **6**, 658.
- 9 S. T. Madrahimov, D. Markovic and J. F. Hartwig, *J. Am. Chem. Soc.*, 2009, **131**, 7228.
- 10 (a) T. Ohshima, Y. Miyamoto, J. Ipposhi, Y. Nakahara, M. Utsunomiya and K. Mashima, *J. Am. Chem. Soc.*, 2009, **131**, 14317; (b) M. Utsunomiya, Y. Miyamoto, J. Ipposhi, T. Ohshima and K. Mashima, *Org. Lett.*, 2007, **9**, 3371; (c) G. Mora, O. Piechaczyk, R. Houdard, N. Mezailles, X.-F. Le Goff and P. le Floch, *Chem.-Eur. J.*, 2008, **14**, 10047; (d) N. D. Knöfel, H. Rothfuss, J. Willenbacher, C. Barner-Kowollik and P. W. Roesky, *Angew. Chem., Int. Ed.*, 2017, **56**, 4950.
- 11 (a) Y. Kita, H. Sakaguchi, Y. Hoshimoto, D. Nakauchi, Y. Nakahara, J.-F. Carpentier, S. Ogoshi and K. Mashima, *Chem.-Eur. J.*, 2015, **21**, 14571; (b) J. B. Sweeney, A. K. Ball, P. A. Lawrence, M. C. Sinclair and L. J. Smith, *Angew. Chem., Int. Ed.*, 2018, **57**, 10202.
- 12 The reuses of Pd complex catalyst and Pt homogeneous catalyst have been carried out<sup>8g,10d</sup>. A. S. Alshammari, K. Natte, N. V. Kalevaru, A. Bagabas and R. V. Jagadeesh, *J. Catal.*, 2020, **382**, 141 and solid catalyst Pd/SiO<sub>2</sub> has been also reported, see:
- 13 (a) K. Masuda, T. Ichitsuka, N. Koumura, K. Sato and S. Kobayashi, *Tetrahedron*, 2018, **74**, 1705; (b) B. Gutmann, D. Cantillo and C. O. Kappe, *Angew. Chem., Int. Ed.*, 2015, **54**, 6688.
- 14 K. Motokura, N. Nakagiri, T. Mizugaki, K. Ebitani and K. Kaneda, *J. Org. Chem.*, 2007, **72**, 6006.
- 15 Y. Kon, T. Nakashima, T. Fujitani, T. Murayama and W. Ueda, *Synlett*, 2019, **30**, 287.
- 16 (a) S. Matsubara, T. Okazoe, K. Oshima, K. Takai and H. Nozaki, *Bull. Chem. Soc. Jpn.*, 1985, **58**, 844; (b) J. Belgacem, J. Kress and J. A. Osborn, *J. Am. Chem. Soc.*, 1992, **114**, 1501; (c) J. D. Burrington, C. T. Kartisek and R. K. Grasselli, *J. Catal.*, 1983, **81**, 489.
- 17 K. Arata, "Preparation of Supercritical Metal Oxides and Their Catalytic Action" *Metal Oxide Catalysis*, Wiley-VCH, Weinheim, 2009, vol. 2.
- 18 For examples; (a) J. Chai, S. Zhu, Y. Cen, J. Guo, J. Wang and W. Fan, *RSC Adv.*, 2017, **7**, 8567; (b) J. S. Lee, J. W. Yoon, S. B. Halligudi, J.-S. Chang and S. H. Jhung, *Appl. Catal., A*, 2009, **366**, 299.
- 19 (a) D. G. Barton, M. Shtein, R. D. Wilson, S. L. Soled and E. Iglesia, *J. Phys. Chem. B*, 1999, **103**, 630; (b) N. Naito, N. Katada and M. Niwa, *J. Phys. Chem. B*, 1999, **103**, 7206; (c) A. Martínez, G. Prieto, M. A. Arribas, P. Concepción and J. F. Sánchez-Royo, *J. Catal.*, 2007, **248**, 288; (d) E. I. Ross-Medgaarden, W. V. Knowles, T. Kim, M. S. Wong, W. Zhou, C. J. Kiely and I. E. Wachs, *J. Catal.*, 2008, **256**, 108.
- 20 (a) Y. Izumi, K. Matsuo and K. Urabe, *J. Mol. Catal.*, 1983, **18**, 299; (b) I. V. Kozhevnikov and K. I. Matveev, *Appl. Catal.*, 1983, **5**, 135.
- 21 Reviews for cationic ion exchange resins, see: A. Chakrabarti and M. M. Sharma, *React. Polym.*, 1993, **20**, 1.
- 22 The 50% conversion of **2** (0.5 mmol) in Table 1, entry 11 was in good accordance with the amounts of active -SO<sub>3</sub>H groups (> 0.47 mmol) in amberlyst 15DRY (100 mg) calculated from the ion exchange capacity (>4.7 mol kg<sup>-1</sup>).
- 23 W surface densities (W nm<sup>-2</sup>) were calculated by the following equation considering the paper from C. Thomas, *J. Phys. Chem. C*, 2011, **115**, 2253 and ref. 19d: W surface density (W nm<sup>-2</sup>) = [(wt% W/100)/M<sub>W</sub> × 6.023 × 10<sup>23</sup>]/[S.A. × 10<sup>18</sup>/(1 - (wt% W/100)) × (M<sub>WO3</sub>/M<sub>W</sub>)].
- 24 K. AlGhamdi, J. S. J. Hargreaves and S. D. Jackson, "Base Catalysis with Metal Oxides" *Metal Oxide Catalysis*, Wiley-VCH, Weinheim, 2009, vol. 2.
- 25 C. D. Wagner, W. M. Riggs, L. E. Davis and J. F. Moulder, *Handbook of X-ray photoelectron spectroscopy*, ed. G. E. Muillemberg, PerkinElmer, Eden Prairie, MN, 1978.
- 26 TOF (h<sup>-1</sup>) was calculated as the following equation: [3 obtained from the allylation of **2** with **1** by passing through a catalyst column for 1 h (mmol)]/[WO<sub>3</sub> in a catalyst column (mmol)].

